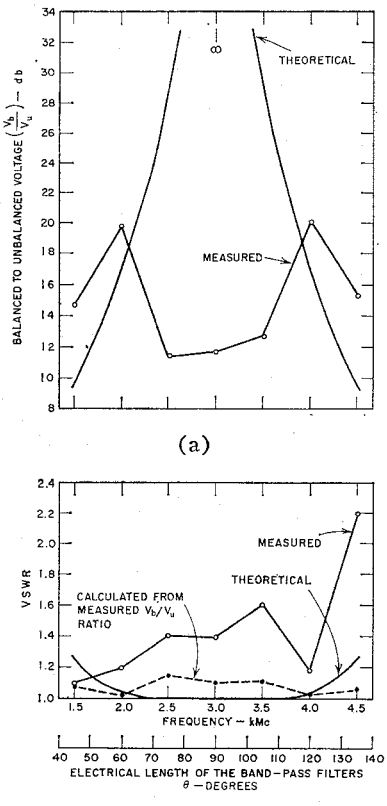

Fig. 12—Experimental performance of strip-line Balun I.

ferred by comparing the measured VSWR in Fig. 12 with the VSWR calculated from the measured V_b/V_u ratio by means of (5) and (6).

Conclusions

The theoretical analysis of these baluns has shown that they have good wide-band performance. The baluns using unstaggered band-pass filters have a very low VSWR over their operating frequency range; in comparison, the baluns using staggered band-pass filters have a higher input VSWR, but a better balance of the output voltage over the same bandwidth. However, in either type of balun the balanced to unbalanced voltage ratio may be greatly increased by inserting a suitably oriented resistance card between the strips connecting to the output ports.

The measured performance of the experimental balun is good over a 3:1 frequency range, although the experimental performance agrees only approximately with theory, because of discontinuity effects. It is believed that, by reducing junction discontinuities, the balun performance can be made to conform closely to the theoretical results.

Acknowledgment

The authors wish to acknowledge the suggestions and help of Dr. S. B. Cohn.

Periodic Structures in Trough Waveguide*

A. A. OLINER† and W. ROTMAN‡

Summary—**The center fin in trough waveguide can be modified in a periodic fashion to alter the propagation characteristics of the guide. Two such periodic modifications, one an array of circular holes and the second a periodic array of teeth, have been measured fairly extensively and analyzed theoretically. These configurations are useful in connection with antenna scanning or waveguide filter applications.**

The array of holes produces only a mild slowing of the propagating wave, but the toothed structure, which may alternatively be described as a series of flat strips extending beyond the edge of the fin, can cause the propagating wave to vary from a very slow to a very fast wave. The periodic structures are theoretically treated by two methods, a transverse resonance procedure and a periodic cell approach. These theoretical results agree very well with each other and with the measured data.

* Manuscript received by the PGMTT, July 14, 1958; revised manuscript received, September 12, 1958. Part of this study was supported by the Air Force Cambridge Research Center under Contract No. AF 19(604)-2031.

† Microwave Res. Inst., Polytechnic Inst. of Brooklyn, Brooklyn, N. Y.

‡ Air Force Cambridge Res. Ctr., Bedford, Mass.

I. Introduction

TROUGH waveguide is a relatively new waveguide type possessing a number of interesting properties. The geometry of the guide is shown in Fig. 1. It is derived from symmetrical strip transmission line by placing a short circuit at the midplane of the latter;[1] for this reason, the dominant mode in trough waveguide is identical with the first higher mode in the strip transmission line. The electric field distribution is indicated in Fig. 1 as being oppositely directed in the top and bottom portions; hence, if the plate spacing in the region beyond the edge of the center fin is less than a half wavelength, the field is of the below cutoff type in this outer region when viewed in the transverse direction. Thus, by virtue of symmetry, one of the guide walls is reactive and the structure is non-radiating.

[1] Airborne Instruments Lab., advertisement on trough waveguide, Proc. IRE, vol. 44, p. 2A; August, 1956.

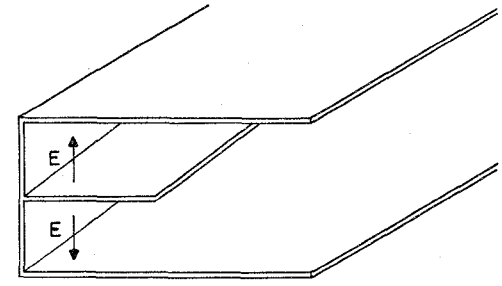

Fig. 1—The trough waveguide.

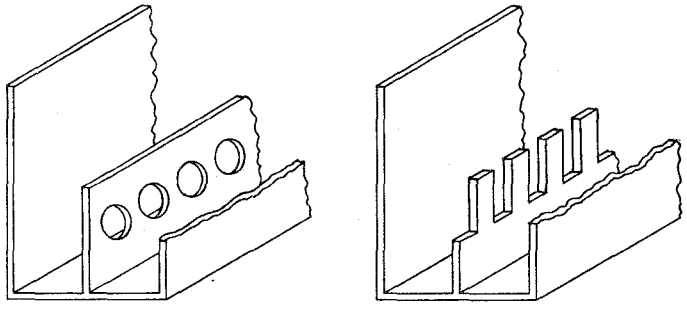

Fig. 2—Two types of periodic structures in trough waveguide. (a) Array of holes. (b) Array of teeth.

The dominant mode in trough waveguide is an H, or TE, mode, with a transverse wavenumber which is independent of frequency. Expressions for the transverse wavenumber, or alternatively the cutoff wavelength, as a function of guide geometry are available both for center fins of zero thickness and for fins of finite thickness.[2]

Trough waveguide possesses three properties of particular interest. First, it can be coupled very smoothly to coaxial line; second, the dominant mode possesses a nominal bandwidth of approximately 3:1, in contrast to the approximately 2:1 value for normal rectangular waveguide; and third, it is an open structure, so that any asymmetry produces radiation. Those features concerned with the large bandwidth and excellent match to coaxial line are useful for a variety of component applications. The open nature of the line lends itself to the design of novel types of line source antennas.[2,3]

Since the variation with frequency of the trough waveguide propagation characteristics is similar to that of an ordinary waveguide, a considerable measure of added versatility is obtained by periodically loading the waveguide. By properly choosing the loading, the wave, which is ordinarily a fast wave, can be made into a slow wave or into an even faster wave, pass and stop bands can be obtained, or rapid variations of propagation constant with frequency can be produced. While periodic loading can produce these effects in many types of waveguiding structures, this loading in trough waveguide can be achieved readily by modifications in the center fin only. In fact, these modifications may be produced, if desired, by photo-etching or stamping techniques. For example, periodic structures in trough waveguide have been employed in antenna rapid scan applications by the Air Force Cambridge Research Center, and in filter applications by the Airborne Instruments Laboratory.

A study of two types of periodic structures in trough waveguide is described in this paper. These two types, which are shown in Fig. 2, are an array of circular holes in the center fin, and a series of flat strips extending beyond the edge of the center fin. For convenience, the second structure will be referred to as an array of teeth. Both types of structures were examined experimentally and analyzed theoretically.

An array of circular holes never produces a heavy loading, and its effect on the trough waveguide is to cause a mild slowing of the wave. The propagation characteristics of the toothed array, on the other hand, are significantly different from those of the unloaded trough waveguide. By proper choice of dimensions, the width and location in frequency of the pass bands may be selected as desired, and the wave may be made fast or slow.

The trough waveguide periodic structures were analyzed theoretically by two methods: a periodic cell approach, and a transverse resonance procedure. In the case of the array of holes, the results of both methods agreed very well with each other and with the measured values. In the case of the array of teeth, the periodic cell approach yields accurate values only when the teeth are far apart, because of the strong mutual coupling between neighboring teeth. For this reason, only the transverse resonance analysis of the array of teeth is included in this paper.[4] This analysis agrees very well with the measured data over a wide range of parameter values.

The theoretical expressions for the propagation characteristics of these periodic arrays are not only accurate but are also in simple and practical form. Numerical values can be readily obtained from them.

In the transverse resonance analysis of the array of teeth, it was necessary, as an intermediate step, to derive an expression for the characteristic impedance of multistrip transmission line. The geometry of this line is indicated in Fig. 11(a) of the appendix, where a simple approximate expression for the characteristic impedance is derived. This simple expression is compared there with a cumbersome rigorous conformal mapping result; the approximate form shows remarkable accuracy over a wide range of dimensions. This intermediate result may also be of value in itself.

[2] W. Rotman and A. A. Oliner, "Asymmetrical Trough Waveguide Antennas," IRE Trans. on Antennas and Propagation, to be published.

[3] W. Rotman and N. Karas, "Some new microwave antenna designs based on the trough waveguide," IRE Convention Rec., part I, pp. 230–235; 1956.

[4] The periodic cell analysis for the toothed array is included in a forthcoming Air Force Cambridge Res. Ctr. Rep. by W. Rotman and N. Karas, "Trough Waveguide Radiators with Periodic Posts."

II. Array of Circular Holes

A. *Periodic Cell Analysis*

The first of the two methods employed for determining the propagation characteristics of trough waveguide loaded by an array of round holes in the center fin is the periodic cell approach. This approach is most suitable for geometries in which the holes are not too closely spaced to each other. However, since the mutual coupling between circular holes is known to be quite small, results obtained with the periodic cell approach should be valid even when the holes are fairly close to each other.

The geometry of the array of holes is indicated in Fig. 3, together with the notation to be employed. As seen, the array need not be centered in the fin.

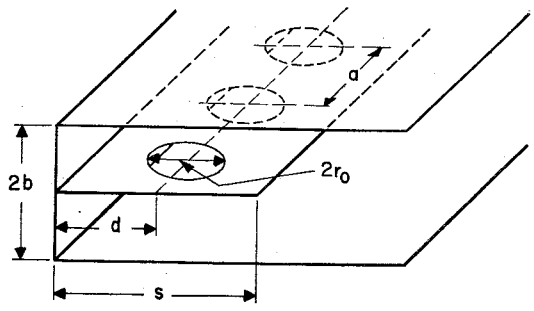

Fig. 3—Geometry of array of circular holes in center fin of trough waveguide.

A view of the center fin alone is shown in Fig. 4(a). The periodic cell approach first requires the choice of a unit cell, which is shown in Fig. 4(a) to lie between reference planes T_1 and T_2. The second step, that of deducing an equivalent network for the unit cell, is indicated in Fig. 4(b). This network is seen to consist of two lengths of unloaded trough waveguide, each equal to one-half the length of the unit cell, and coupled together at the midplane of the unit cell by an equivalent circuit for the circular hole by itself. The third step in the procedure is indicated by Fig. 4(c); it consists of obtaining a smooth transmission line equivalent to the original periodically loaded line. This equivalence is valid only at the accessible reference planes T_1 and T_2, of course. The unloaded trough waveguide and the equivalent smooth line are characterized, respectively, by propagation wavenumbers $\kappa_0 (= 2\pi/\lambda_{go})$ and $\hat{\kappa}$, and characteristic admittances Y_o and $\hat{Y}$. The quantity of final interest is the equivalent macroscopic guide wavelength λ_g of the periodically loaded trough waveguide, and this quantity is, of course, related to $\hat{\kappa}$ by

$$\lambda_g = 2\pi/\hat{\kappa}. \tag{1}$$

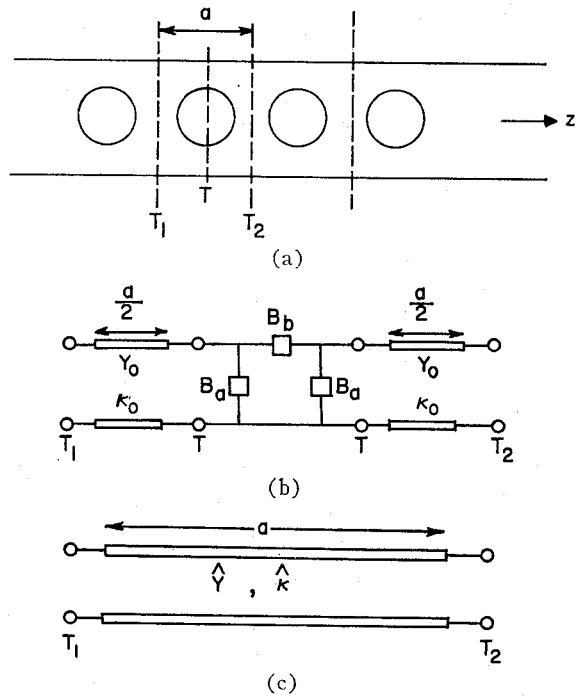

Fig. 4—Development of periodic cell analysis for array of holes. (a) View of center fin. (b) Equivalent network of unit cell. (c) Equivalent smooth transmission line.

One method of obtaining equivalence at reference planes T_1 and T_2 between the composite equivalent network of Fig. 4(b) and the equivalent smooth transmission line of Fig. 4(c) is by the use of bisection theorems, taking advantage of the symmetry of the networks. Each of the two networks is bisected and short circuit and open circuit terminations are placed successively at the midplanes. The corresponding input admittances to each network are then equated; the following relation is obtained as a result:

$$\cos \hat{\kappa} a = \left[\frac{B_a' + B_b'}{B_b'}\right] \cos \kappa_0 a + \frac{1}{2B_b'} [1 - B_a'(B_a' + 2B_b')] \sin \kappa_0 a, \tag{2}$$

where B_a' and B_b' are the pi network parameters at centerline reference plane T of a single round hole in trough waveguide, normalized to the characteristic admittance Y_o of the unloaded guide. From (2) and (1) one readily calculates the guide wavelength λ_g of ultimate interest.

Before numerical results can be computed, however, expressions are needed for B_a' and B_b'. Such expressions were derived from general small aperture relations for a symmetrical longitudinal aperture,[5] the latter being obtained by a generalization of well-known results for transverse apertures. The resulting expressions are

$$B_b' = -\frac{3b\lambda_{go}}{k_{co}(4r_o)^3 \sin^2 k_{co}d} \tag{3}$$

$$B_a' = \frac{\lambda_{go}(2k_{co}r_o)^3 \cos^2 k_{co}d}{3\pi^2 b} \cdot \left[1 - \frac{1}{2}\left(\frac{k}{k_{co}}\right)^2 \tan^2 k_{co}d\right], \tag{4}$$

[5] A. A. Oliner, "Equivalent Circuit for Round Hole in Trough Waveguide," Memorandum No. 38, R-645-58, PIB-573, Microwave Res. Inst., Polytechnic Institute of Brooklyn, Brooklyn, N. Y.; February, 1958.

where most of the symbols are indicated in Fig. 3. Lengths r_o, d, and $2b$ are seen to be the hole radius, the distance from the center of the hole to the side wall of the guide, and the spacing between the top and bottom plates, respectively. Quantity k $(=2\pi/\lambda)$ is the free space wavenumber, λ_{go} is the guide wavelength of the unloaded trough waveguide, and k_{co} $(=2\pi/\lambda_{co})$ is the cutoff wavenumber of the unloaded guide, and is related to κ_0 in (2) by

$$\kappa_0 = \sqrt{k^2 - k_{co}^2}. \tag{5}$$

The cutoff wavelength λ_{co} for a zero-thickness center fin may be obtained either from a curve[2] or from the following transcendental relation:

$$\frac{\lambda_{co}}{4b} = \frac{s}{b} + \frac{2}{\pi}\ln 2 + \frac{\lambda_{co}}{2\pi b} S_1\left(\frac{4b}{\lambda_{co}}\right) - \frac{\lambda_{co}}{\pi b} S_1\left(\frac{2b}{\lambda_{co}}\right), \tag{6}$$

where S_1 is the rapidly convergent arcsine sum

$$S_1(x) = \sum_{n=1}^{\infty}\left(\sin^{-1}\frac{x}{n} - \frac{x}{n}\right). \tag{7}$$

The contributions from the arcsine sums are relatively small, although they are not negligible. For the range $s/b>1$, the arcsine sums contribute less than 3 per cent to the value of λ_{co}/b.

With the knowledge of λ_{co}, κ_0 can be found readily from (5), and B_b' and B_a' from (3) and (4). The substitution of these quantities into (2) then permits the determination, via (1), of the guide wavelength λ_g of the periodically loaded structure.

B. *Transverse Resonance Procedure*

The second method used for analyzing the array of holes is the transverse resonance procedure. The limitation in the applicability of the transverse resonance procedure is that the holes must not come too near to the edge of the fin or to the wall contacting the other side of the fin.

The transverse transmission direction, along which the resonance is performed, is taken in the guide cross section along the plane of the center fin. This direction is indicated in Fig. 5(a) as the x direction. As a simplification in the form of the transverse equivalent network, the fringing field at the edge of the fin is replaced in a rigorous manner by an extension l of the center fin and by a magnetic wall termination. The resulting transverse equivalent network, which parallels the structure of Fig. 5(a), is shown in Fig. 5(b). The lengths of line in Fig. 5(b) are characterized by the transverse wavenumber k_t and characteristic admittance Y_t, while the pi equivalent circuit parameters B_a and B_b represent the influence of the array of holes on the transversely propagating wave. This transversely propagating wave consists of two TEM waves, one in the upper and one in the lower parallel plate region, with oppositely directed electric fields and incident at an arbitrary "angle" on

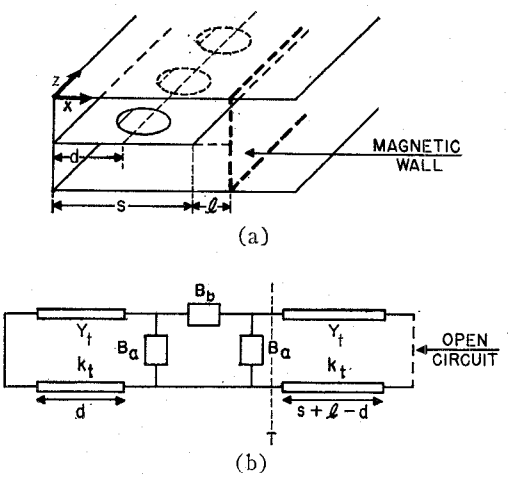

Fig. 5—Transverse resonance analysis of array of holes. (a) Array of holes. (b) Transverse equivalent network.

the array of holes. This angle is a means by which k_t is specified (it is given by $k_t=k\cos\theta$, if θ is the angle of incidence). The equivalent circuit that represents such a wave incident on the array of circular holes has been determined by means of small aperture relations to be:

$$B_b' = -\frac{1}{k_t}\left(\frac{3ab}{8r_o^3}\right) \tag{8}$$

$$B_a' = \left(\frac{2r_o^3}{3ab}\right)\left(\frac{k^2}{k_t} - 2k_t\right), \tag{9}$$

where the parameters are normalized to the characteristic admittance Y_t. The geometrical quantities r_o, a and b are indicated in Fig. 3, and $k(=2\pi/\lambda)$ is the free space wavenumber.

The transverse resonance relation is obtained by equating to zero the sum of the input admittances seen looking in both directions away from some reference plane, chosen as T for convenience, in the equivalent network of Fig. 5(b). One finds as a result the transcendental equation

$$\tan k_t(s - d + l) + B_a' + B_b'\left[\frac{B_a' - \cot k_t d}{B_b' + B_a' - \cot k_t d}\right] = 0, \tag{10}$$

where

$$l = \frac{2b}{\pi}\ln 2 + \frac{1}{k_t}S_1\left(\frac{2k_t b}{\pi}\right) - \frac{2}{k_t}S_1\left(\frac{k_t b}{\pi}\right), \tag{11}$$

and S_1 has been defined in (7). When one substitutes for B_b' and B_a' from (8) and (9), expression (10) becomes rather involved. Since the influence of the array of holes is small, however, it is appropriate to employ a perturbation procedure, by perturbing about the solution for the unloaded guide. The transverse wavenumber k_{co} for the unloaded guide depends only on the guide geometry, as seen from relation (6); for the loaded guide,

the transverse wavenumber k_t is seen to depend on wavelength also, in view of the dependence of B_a' on k in (9).

For the perturbation procedure, one writes

$$k_t = k_{co} + \Delta k_t, \tag{12}$$

and approximates l by l_o, which can be done with negligible error. In addition, use is made of the resonance relation for the unloaded trough waveguide, which may be written as

$$s + l_0 = \frac{\pi}{2k_{co}} \tag{13}$$

for the lowest mode. Relations (12), (8) and (9) are then substituted into (10), and (13) is employed to simplify the resulting form. After some algebra, one finds

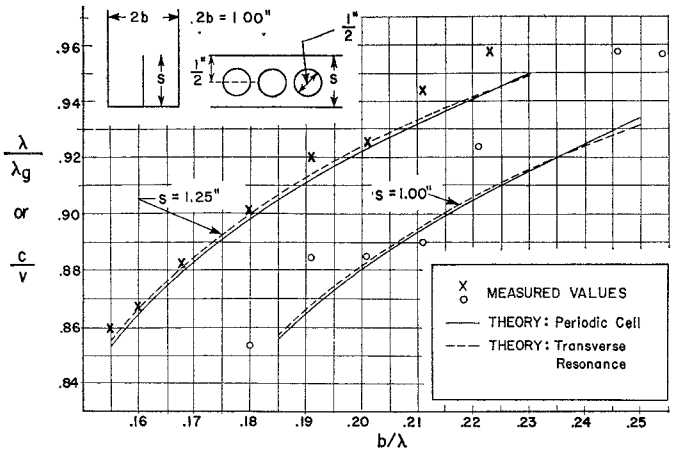

Fig. 6—Propagation characteristics of trough waveguide with an array of circular holes in the center fin.

$$\frac{\Delta k_t}{k} = \frac{1 - \frac{1}{2}\left(\frac{k}{k_{co}}\right)^2 - \cot^2 k_{co}d}{\frac{\pi k}{2k_{co}^2}\csc^2 k_{co}d\left[\frac{3ab}{8r_0^3} - \frac{2r_0^3}{3ab}(k^2 - 2k_{co}^2)\right] - \left(\frac{k}{k_{co}}\right)^3 + \cot k_{co}d \csc^2 k_{co}d\left(\frac{\pi k}{2k_{co}} - 2kd\right)}. \tag{14}$$

In order to relate Δk_t to the guide wavelength λ_g of the periodically loaded guide, one first recognizes that

$$\frac{\lambda}{\lambda_g} = \sqrt{1 - \left(\frac{k_t}{k}\right)^2}. \tag{15}$$

Relation (12) is then substituted into (15); after simplification one finds

$$\frac{\lambda}{\lambda_g} = \frac{\lambda}{\lambda_{go}} - \frac{\lambda_{go}}{\lambda_{co}}\frac{\Delta k_t}{k}, \tag{16}$$

where $\Delta k_t/k$ is given by (14), λ_{co} by (6), and λ_{go} $(=2\pi/\kappa_o)$ by (5).

C. *Comparison with Measurement*

Measurements were taken of the guide wavelengths as a function of frequency for two different trough waveguides, each loaded with a periodic array of circular holes. These measurements are compared in Fig. 6 with theoretical values obtained from both the periodic cell and transverse resonance approaches discussed in Sections A and B. The measured values are indicated as individual points; a certain scatter appears in the data but it should be noted that the ordinate scale is greatly expanded. It is also seen that the theoretical values obtained from the two different approaches agree extremely well with each other. The agreement with the measured values is also good. The close agreement found between the two sets of theoretical values occurs because the measured structures still lie within the approximations inherent in both theoretical approaches; the range of applicable dimensions is increased because circular holes do not couple strongly to their environment.

It is recognized that

$$\frac{\lambda}{\lambda_g} = \frac{c}{v}, \tag{17}$$

where v is the phase velocity of the wave in the loaded guide while c is the velocity in free space. The curves were plotted in the form λ/λ_g to indicate that in this range the waves are still fast waves.

III. Array of Teeth

As indicated in the introduction, only the transverse resonance analysis will be presented for this structure because of the strong mutual coupling between neighboring teeth.

A. *Transverse Resonance Analysis*

The geometry of the array of teeth located on the center fin of trough waveguide is shown in Fig. 7(a). The transverse transmission direction, along which the transverse resonance is performed, is again in the direction shown as x in Fig. 7(a), as in the case of the array of holes. The form of the transverse equivalent network is not as straightforward in this case, however. The form shown in Fig. 7(b) is an approximate one, but one which is capable of high accuracy, nevertheless.

The transversely propagating wave is different in character in the two regions, one of width s and the other of width h. In the former region, the wave is similar to that for the case of the array of holes; it consists of two component TEM waves, one in the upper and one in the lower parallel plate region, with oppositely directed electric fields and traveling together at an

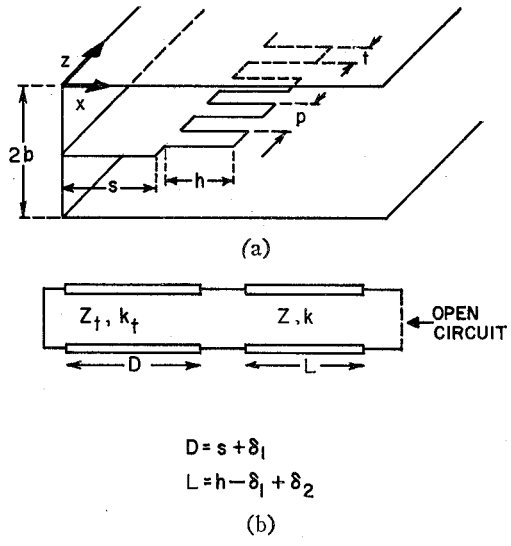

Fig. 7—Transverse resonance analysis of array of teeth. (a) Array of teeth. (b) Transverse equivalent network.

arbitrary angle with respect to the x direction. This angle is alternatively represented by the fact that the wavenumber k_t is different from k. The second region, whose cross-section is shown in Fig. 11(a) of the appendix, can be designated as a multistrip transmission line region. In this region, the transversely propagating wave is constrained to travel in the x direction, so that the wavenumber becomes equal to k. The resonance of the transverse equivalent network yields the resultant value of k_t.

The approximation in the network of Fig. 7(b) occurs in the representation of the junction between the line characterized by Z_t and k_t and that by Z and k. This junction is very difficult to analyze theoretically, and one rigorous representation for it specifies the locations of the input and output reference planes and includes an ideal transformer between them. The approximation employed here sets the transformer turns ratio equal to unity and places the input and output reference planes at the same location; these planes are not located at the physical junction plane, as would occur if the junction effect were negligible, but rather are both shifted a distance δ_1 into the multistrip region. This choice of approximation was motivated by the fact that this form is actually rigorously correct for a certain junction which is a simplification of the structure obtained by taking the Babinet dual of the actual junction. The ultimate justification for the approximation lies in the ability of the network to agree with the measured data; as will be seen below, this postulated simple form is quite accurate.

As indicated by the network of Fig. 7(b), compensation for the fringing field at the edge of the multistrip region is made by extending the strips a distance δ_2 and terminating them by a magnetic wall. The same type of compensation for the fringing field was performed for the edge of the fin in the case of the array of holes. However, since the structures are different the amounts of shift are different, and for the multistrip line the value is not known.

The resonance relation is obtained readily from the network of Fig. 7(b) by choosing a convenient reference plane and equating to zero the sum of the input impedances seen looking in both directions away from the reference plane. One finds for the resonance relation

$$\tan k_t D = \frac{Z}{Z_t} \cot kL, \tag{18}$$

where the symbols are defined in Fig. 7(b). The ratio of characteristic impedances occurring in (18) is evaluated in the appendix; substitution of this result into (18) yields

$$\tan k_t D = \frac{k_t}{k}\left[1 + \frac{p}{\pi b} \ln \csc \frac{\pi t}{2p}\right] \cot kL, \tag{19}$$

where the new symbols are defined in Fig. 7(a). Eq. (19) is seen to be a simple transcendental equation for k_t. When the resultant wave propagating along the loaded trough waveguide is a fast wave, k_t is real. When this wave is a slow wave, however, k_t is imaginary and (19) takes the form

$$\tanh |k_t| D = \frac{|k_t|}{k}\left[1 + \frac{p}{\pi b} \ln \csc \frac{\pi t}{2p}\right] \cot kL. \tag{20}$$

The guide wavelength λ_g of the resulting wave propagating along the loaded trough waveguide (in the z direction) is then obtained from (15).

Before numerical values can be obtained from (19) or (20), the values of δ_1 and δ_2 occurring in D and L must be specified. Since the theoretical determination of these quantities seems a formidable task, an empirical procedure was used for their evaluation. It is first recognized that for a very slow wave the propagation characteristics are essentially independent of the value of D, as seen from (20). Hence, by comparing the theoretical and experimental values of λ/λ_g for a very slow wave situation, the value of $\delta_2 - \delta_1$ can be determined. Once this is known, δ_1 is found by proceeding similarly for a wave which is very fast, using (19) rather than (20). The actual experimental points to which comparison was made are the two extreme points on the $s/b = 1.25$ curve of Fig. 8. The values of δ_1 and δ_2 obtained from these two points are $\delta_1 = .26$, $\delta_2 = .22$. All of the theoretical curves of Figs. 8, 9, and 10 were computed using these two values.

B. *Comparison with Measurement*

Measurements of the propagation characteristics of trough waveguide loaded by an array of teeth attached to the center fin were made over a rather wide range of dimensional values and frequencies. The results of these measurements are plotted as individual points on Figs.

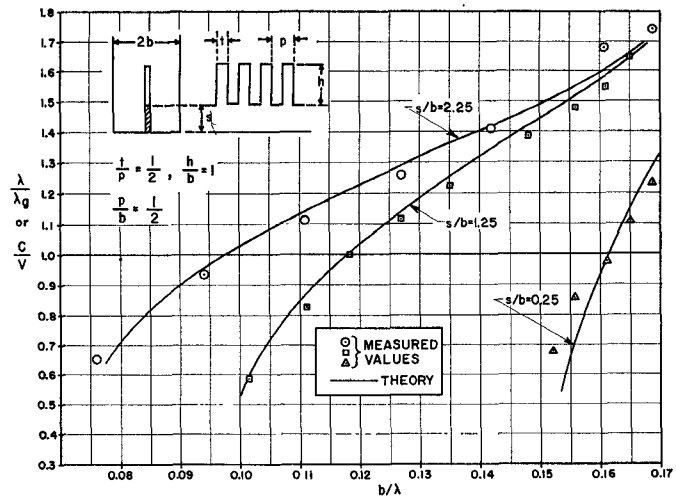

Fig. 8—Effect of center fin width on guide wavelength of periodically toothed trough waveguide.

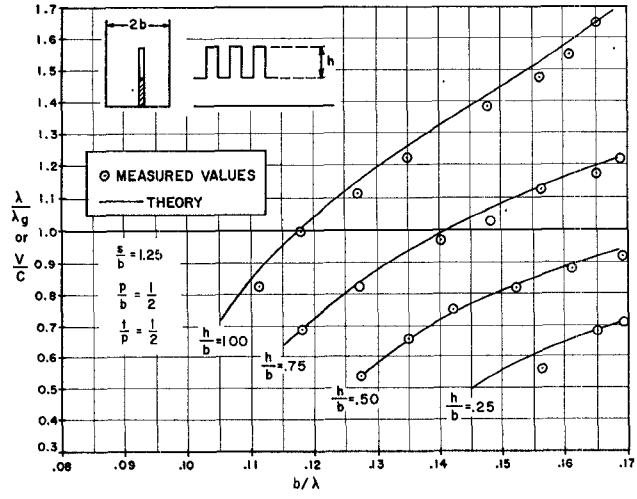

Fig. 9—Effect of tooth height on guide wavelength of periodically toothed trough waveguide.

8, 9, and 10. Although the abscissa scale is labeled b/λ, b was maintained constant throughout the series of measurements.

The corresponding theoretical values appear on these figures as solid lines. These values are computed from (19) or (20) together with (15), and in all cases the values of δ_1 and δ_2 discussed above were employed. Very good agreement can be noted between the measured and theoretical values for all cases. This order of agreement over such a wide range of parameter values testifies to the correctness of the postulated simple form for the transverse equivalent network of Fig. 7(b). It should also be noted that this simple form permits a rapid calculation of the propagation characteristics.

Since the λ/λ_g or c/v values in Figs. 8, 9, and 10 range both above and below unity, the wave can be either slow or fast. Furthermore, as seen in Fig. 8, the slope of the curve can be varied considerably, yielding a narrow pass band, if desired. The versatility exhibited in Fig. 8 is obtained by changing only the width s of the supporting fin; a smaller center fin yields a narrower pass band. From Fig. 9, one notes that large variations in performance follow from changes in the lengths h of the teeth. In Fig. 10 it is seen that changes in the periodicity of the teeth tend to lift the whole curve up or down. The lowest curve of Fig. 10 corresponds to the case for which the teeth are absent; the effect of the teeth is seen to be quite significant.

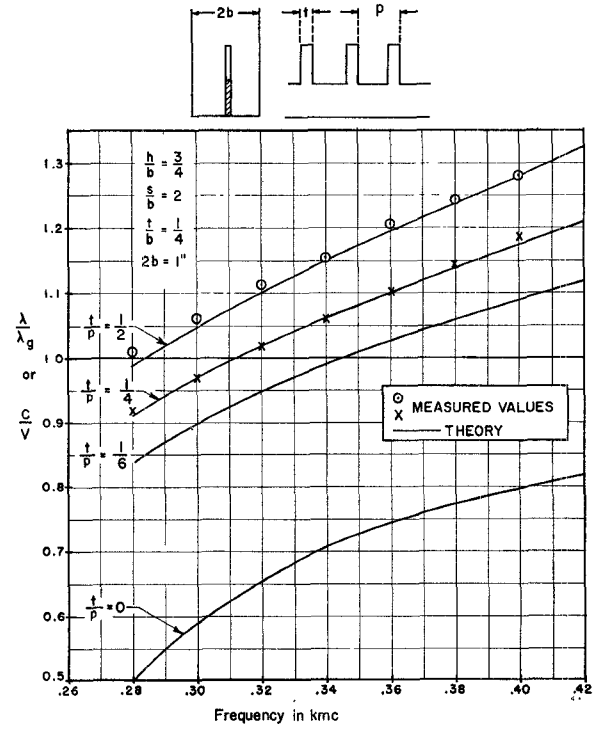

Fig. 10—Effect of tooth spacing on guide wavelength of periodically toothed trough waveguide.

Appendix

Characteristic Impedance of Multistrip Transmission Line

The toothed region of the trough waveguide loaded by the periodic array of teeth when viewed in the transverse direction has been designated as a multistrip transmission line. In the derivation of the transverse resonance relation for this structure it is necessary to have available a simple analytical expression for the characteristic impedance of this multistrip line. A rigorous conformal mapping result can be obtained but it is too cumbersome for use in the transverse resonance relation. However, a simple but highly accurate expression is derived in the manner described below.

A cross section of the multistrip line is shown in Fig. 11(a), together with typical electric field lines and a unit cell to indicate the periodic nature of the structure. In Fig. 11(b), this unit cell is shown bisected, enlarged, and placed on its side. From symmetry, the unit cell is bounded by magnetic walls as shown; the distribution of magnetic field lines in the cell is also indicated in the figure. The bisected unit cell can be represented by the equivalent network in Fig. 11(c), in which the distortion

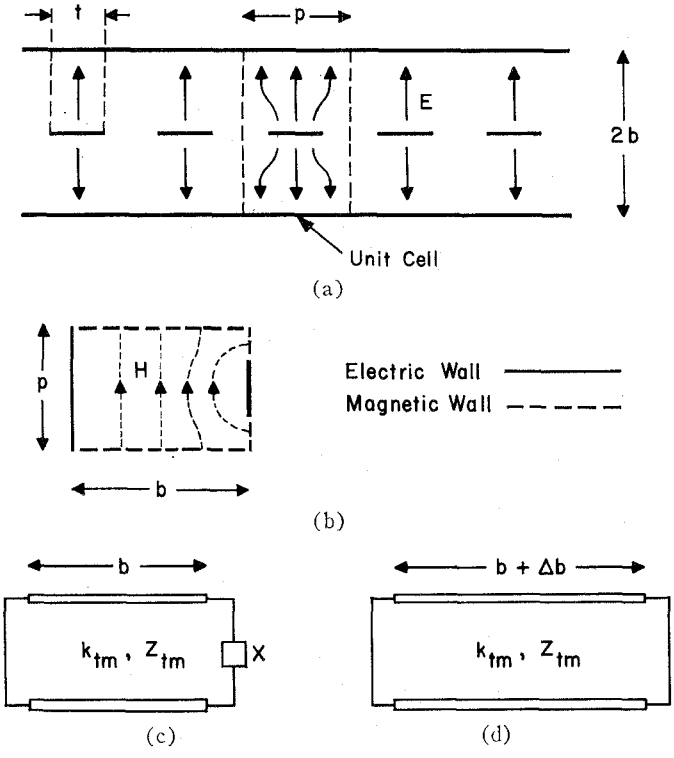

Fig. 11—Development of network representation for unit cell of multistrip transmission line. (a) Cross section, showing unit cell and electric field lines. (b) Bisected unit cell placed on its side, showing magnetic field lines. (c) Equivalent network representing bisected unit cell. (d) Simplified equivalent network with modified length of line.

of the field lines is accounted for by the reactance X. Since the reactance is equivalent to a short-circuited length of line, this equivalent network can be replaced by the simplified one of Fig. 11(d), which involves a modification in the line length. The additional length Δb of line is then related to the normalized reactance X' by

$$\tan k_{tm}\Delta b = X', \tag{21}$$

where k_{tm} represents the transverse wavenumber of the multistrip line.

The reactance X' can be evaluated by employing a Babinet equivalence. The original structure, taken from the unit cell, is shown in Fig. 12(a), while its Babinet dual structure is given in Fig. 12(b). It is noted that in the duality process the magnetic and electric walls are interchanged, and the magnetic field lines of the original structure become the electric field lines of the dual structure. The dual structure is readily seen to be a bisected capacitive slit whose normalized susceptance B' is given by[6]

$$B' = \frac{k_{tm}p}{\pi} \ln \csc \frac{\pi t}{2p}, \tag{22}$$

since the guide wavelength of the wave "incident" on the slit is $\lambda_{tm}(=2\pi/k_{tm})$. But, by the Babinet equivalence,

[6] N. Marcuvitz, "Waveguide Handbook," Rad. Lab. Ser., vol. 10, McGraw-Hill Book Company, Inc., New York, N. Y., p. 218, eq. 2(a); 1951. Only the static contribution of 2(a) is used.

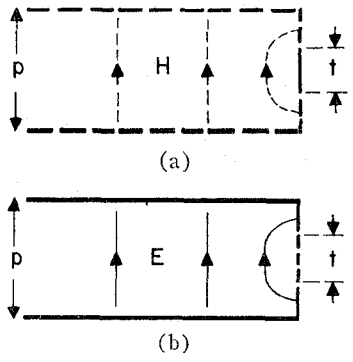

Fig. 12—Reactance structure and its Babinet dual. (a) Reactance structure. (b) Babinet dual structure.

the normalized reactance X' of the original structure is equal to B' of (22). Furthermore, since k_{tm} is the transverse wavenumber of a TEM mode (along the multistrip line), $k_{tm}=0$. Thus, in relation (21), the tan can be replaced by its argument, the k_t values cancel when (22) is employed for X', and one obtains

$$\Delta b = \frac{p}{\pi} \ln \csc \frac{\pi t}{2p}. \tag{23}$$

The characteristic impedance of the bisected unit cell represented by the network of Fig. 11(d) is

$$Z_b = 120\pi \frac{b + \Delta b}{p}. \tag{24}$$

From Fig. 11(a) it is seen that the unbisected unit cell consists of two bisected cells in parallel, so that the characteristic impedance Z of the complete unit cell is

$$Z = 30\pi \left[\frac{2b}{p} + \frac{2}{\pi} \ln \csc \frac{\pi t}{2p} \right], \tag{25}$$

after substitution is made for Δb from (23).

The application to the transverse resonance relation (18) requires not Z alone, but its ratio to Z_t, the characteristic impedance of the structure obtained when the array of center strips of Fig. 11(a) is replaced by a continuous conducting sheet, but for a wave traveling in the direction of the strips with wavenumber k_t rather than k. The value of Z_t, normalized to the same unit cell, is given by

$$Z_t = 30\pi \frac{2b}{p} \frac{k}{k_t}, \tag{26}$$

since the propagating mode is an H mode. From (25) and (26) one obtains finally

$$\frac{Z}{Z_t} = \frac{k_t}{k} \left[1 + \frac{p}{\pi b} \ln \csc \frac{\pi t}{2p} \right]. \tag{27}$$

Relation (27) was the form employed for Z/Z_t in the step from (18) to (19).

The variation of the bracketed quantity in (27) with $2b/p$ is shown in Fig. 13, with t/p as a parameter. For

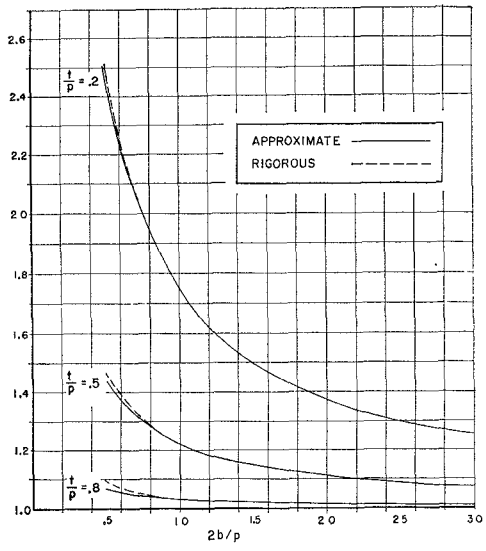

Fig. 13—Theoretical values for the characteristic impedance of multistrip line.

wide strips this quantity is nearly unity. Also included in Fig. 13 is the corresponding result obtained from a rigorous conformal mapping.[7] The rigorous result is too cumbersome in form to be useful in the transverse resonance procedure, but one sees from the comparison in Fig. 13 that the approximate result (27) is extremely accurate over a wide range of parameter values. It is also interesting that in the range in which the two results begin to disagree, the accuracy of the tables required for the rigorous result becomes poor, so that asymptotic expressions must be employed for the functions involved and the rigorous result becomes more difficult to compute from. However, in this range the geometric proportions of the multistrip line are such that other approximations become suitable.

[7] C. A. Hachemeister, "The Impedance and Fields of Some TEM Mode Transmission Lines," Rep. R-623-57, PIB-551, Microwave Res. Inst., Polytechnic Institute of Brooklyn, N. Y.; April 16, 1958.

A Study of a Serrated Ridge Waveguide*

H. S. KIRSCHBAUM† AND R. TSU‡

Summary—**The serrated, or periodically slotted ridge produces a periodic loading which retards the phase velocity of the wave in a waveguide. Such structures may be used to provide a variable index of refraction for microwave lenses and as elements in microwave filters. Two approaches are presented in this paper giving the frequency dependence of the index of refraction. One is based on equivalent circuit representations which are qualitatively valid for the effect of the loading. Circuit parameters which determine the shape of the index of refraction curve are calculated from the experimental data. The other approach providing a purely analytic expression of the index of refraction is derived by a field matching method. Calculations show good agreement with test data.**

Introduction

A SERRATED ridge waveguide is a ridge waveguide with slots cut periodically in the ridge, the slots being transverse to the direction of propagation. The periodicity of the slotting is very small compared to the width of the waveguide, being about 12 per cent of the guide width for those cases studied experimentally.

The purpose of slotting the ridge is to add reactive loading in the guide in order to decrease the phase velocity of the wave. The degree of reduction in phase-velocity depends upon the degree of loading. Such a structure can be used as a means of obtaining a large range of refractive index for use in microwave lenses.[1,2] It may also be used in microwave filter circuitry.

This paper presents a description of two approaches to the evaluation of the index of refraction from the significant dimensions of the guide and its ridge. The first of these is a heuristic approach which seeks to explain the behavior of the guide on the basis of physical reasoning. This leads to two possible transmission line equivalences for the serrated ridge guide, from which the index of refraction can be calculated. This is essentially a semiempirical approach. It enables one to extend the range of knowledge about this structure through the performance of a few judiciously chosen experiments. The second approach involves an attempt to solve the wave equation for the propagation constant in the axial direction of the guide, through the expedient of field

* Manuscript received by the PGMTT, May 23, 1958; revised manuscript received, August 4, 1958. The work described was done, in part, under contract between The Ohio State Univ. Res. Found. and the Sperry Gyroscope Co., Div. of Sperry Rand Corp., Great Neck, L. I., N. Y.

† Battelle Memorial Inst., Columbus, Ohio. Formerly The Ohio State University, Columbus, Ohio.

‡ The Ohio State University, Columbus, Ohio.

[1] R. L. Smedes, "High efficiency microwave lens," *Sperry Eng. Rev.*, vol. 9, pp. 1–10; May–June, 1956.

[2] E. K. Proctor, "Methods of reducing chromatic aberration in metal plate microwave lenses," IRE TRANS. ON ANTENNAS AND PROPAGATION, vol. AP-6, pp. 231–239; July, 1958.